Available online at www.sciencedirect.com
ScienceDirect
Nuclear Physics A 931 (2014) 1103–1107
NUCLEAR PHYSICS A
www.elsevier.com/locate/nuclphysa

Light (hyper-)nuclei production at the LHC measured with ALICE

Nicole Martin [a,b,*] (for the ALICE Collaboration) [1]

[a] *ExtreMe Matter Institute EMMI and Research Division, GSI Helmholtzzentrum für Schwerionenforschung, Darmstadt, Germany*
[b] *Institut für Kernphysik, Technische Universität Darmstadt, Darmstadt, Germany*

Received 31 July 2014; received in revised form 5 September 2014; accepted 6 September 2014

Abstract

The high collision energies reached at the LHC lead to significant production yields of light (hyper-)nuclei in proton–proton, proton–lead and, in particular, lead–lead collisions. The excellent particle identification capabilities of the ALICE apparatus, based on the specific energy loss in the Time Projection Chamber and the velocity information in the Time-Of-Flight detector, allow for the detection of these rarely produced particles. Results on the production of stable nuclei in p–Pb and Pb–Pb collisions are presented. Hypernuclei production rates in Pb–Pb interactions are also shown and upper limits for the production of lighter exotica candidates. All results are compared with predictions obtained using thermal (statistical) and coalescence models.

Keywords: Nuclei; Hypertriton; Exotic bound states

1. Introduction

The collision energy reached at the LHC provides the opportunity to measure nuclei and hypernuclei and the corresponding anti-particles in unprecedented abundances, although the measurement is challenging as the production probability decreases with increasing mass. The results

---

[*] Correspondence to: ExtreMe Matter Institute EMMI and Research Division, GSI Helmholtzzentrum für Schwerionenforschung, Darmstadt, Germany.

[1] A list of members of the ALICE Collaboration and acknowledgments can be found at the end of this issue.

http://dx.doi.org/10.1016/j.nuclphysa.2014.09.017
0375-9474/

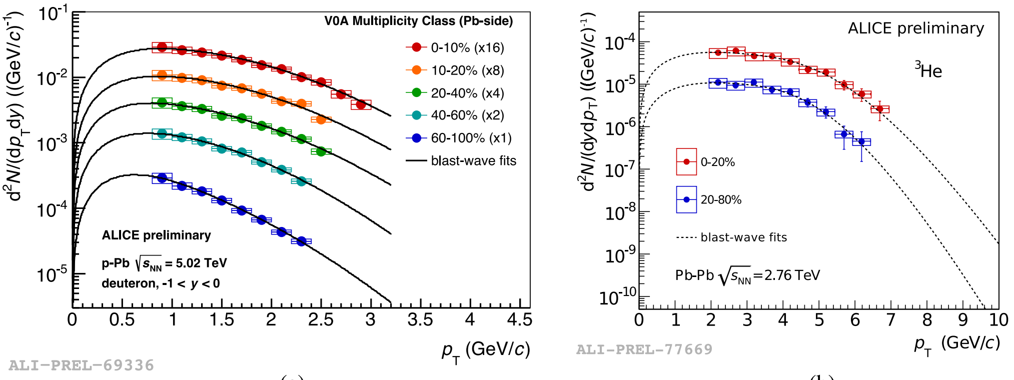

(a) (b)

Fig. 1. Transverse momentum spectra in different multiplicity classes for deuterons in p–Pb (a) and for different centrality bins for ^{3}He in Pb–Pb (b).

presented here are obtained with the data of Pb–Pb collisions at $\sqrt{s_{NN}} = 2.76$ TeV recorded in two periods during the years 2010 and 2011 and p–Pb collisions at $\sqrt{s_{NN}} = 5.02$ TeV recorded at the beginning of 2013. Due to its unique particle identification capabilities the ALICE detector system [1] is ideally suited to measure the rarely produced nuclei and hypernuclei and for the search of exotic states like a possible Λn bound state and the H-dibaryon. In terms of models, to describe the production mechanism of these particles two different approaches are considered. In the thermal model [2,3] the chemical freeze-out temperature T_{chem} is the key parameter at LHC energies. The production yields depend exponentially on this temperature and the mass m: $\mathrm{d}N/\mathrm{d}y \sim \exp(-m/T_{\text{chem}})$. Due to their large masses the abundance of nuclei is very sensitive to T_{chem}. In the coalescence approach nuclei are formed at the kinetic freeze-out by protons and neutrons which are nearby and have similar velocities.

2. Nuclei

Nuclei are identified using the specific energy loss ($\mathrm{d}E/\mathrm{d}x$) measurement in the Time Projection Chamber (TPC) [4]. They are selected in a 3σ range around the theoretical curves described by the Bethe–Bloch formula [5]. Since these curves start to overlap at high momenta, the velocity measurement with the Time-Of-Flight detector (TOF) [1] is used in addition to allow for clear identification. The measured raw spectra are corrected for efficiency and acceptance. As an example, Fig. 1 shows the deuteron transverse momentum p_T spectra in different multiplicity classes in p–Pb collisions (left panel) (the multiplicity classes are explained in [6]) and the ^{3}He spectra for two centrality bins in Pb–Pb collisions (right panel). For deuteron spectra in Pb–Pb collisions see [7]. The spectra show a hardening with increasing multiplicity/centrality and are fitted with individual blast-wave functions. Fig. 2 shows the deuteron-to-proton ratio as a function of the multiplicity in pp, p–Pb and Pb–Pb. The ratio rises with multiplicity until a saturation within errors in Pb–Pb collisions is reached.

Another way of representing this quantity is via the coalescence parameter $B_2 = E_{\text{deuteron}} \times \frac{d^3N_{\text{deuteron}}}{dp^3_{\text{deuteron}}} / \left(E_{\text{proton}} \frac{d^3N_{\text{proton}}}{dp^3_{\text{proton}}}\right)^2$. Fig. 3 shows B_2 for p–Pb and Pb–Pb collisions. In a simple coalescence model, B_2 is independent of p_T. This is observed in p–Pb and peripheral Pb–Pb. In second order B_2 scales like the HBT radii [8] and therefore, the decrease with centrality in

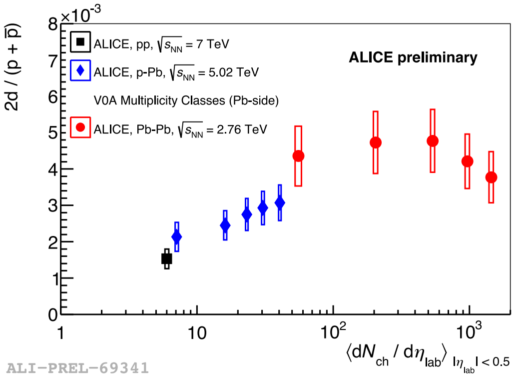

Fig. 2. Deuteron-to-proton ratio as a function of charged-particle multiplicity at midrapidity.

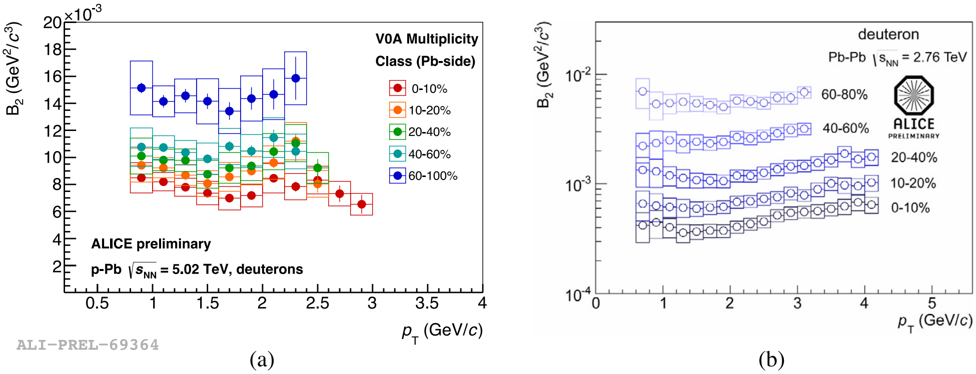

(a) (b)

Fig. 3. Coalescence parameter B_2 as a function of p_T for deuterons in p–Pb (a) and in Pb–Pb (b) collisions.

Pb–Pb is understood as an increase in the source volume and the p_T-slope which develops in central Pb–Pb reflects the k_T-dependence of the homogeneity volume in HBT.

3. Hypertriton

The production of hypertriton ${}^{3}_{\Lambda}H$ has been measured in Pb–Pb collisions via invariant mass reconstruction in the decay channel ${}^{3}He + \pi^{-}$. The hypertriton has a mass of 2.991 ± 0.002 GeV/c^2 and a decay length on the order of that of the free Λ particle. Hypertriton candidates are identified via their weak decay in invariant mass distributions which are reconstructed for two tracks originating from a secondary vertex, where one is identified as a ${}^{3}He$ and the second one as a pion via the TPC dE/dx information. The resulting invariant mass distributions are shown for example in [9]. As the production yield dN/dy depends on the branching ratio (B.R.), the dN/dy is compared to different models as a function of the B.R. in Fig. 4(a). For the most likely B.R. of 25% [10] the measured dN/dy agrees very well with the equilibrium thermal model prediction for 156 MeV [11].

When the measured deuteron, ${}^{3}He$, and hypertriton yields are included in a thermal fit [12] (based on [2]) in addition to lighter particles, the resulting T_{chem} does not change (for a recent fit of the ALICE measurements without the nuclei and the hypertriton see for instance [12,13]).

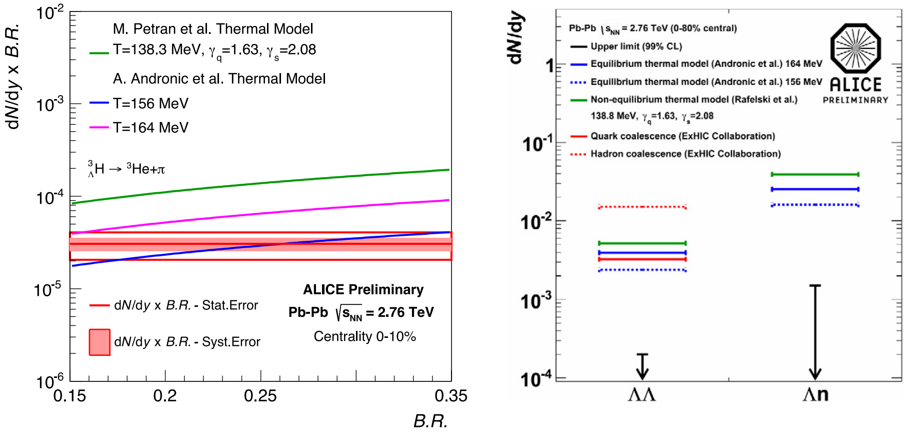

(a) (b)

Fig. 4. dN/dy comparison to different models for the hypertriton measurement (a) and for the $\Lambda\Lambda$ and Λn bound state (b).

As shown in [12] the measured yields of the nuclei and the hypertriton agree very well to the fit values.

4. Exotic bound states

Searches for the H-dibaryon and the Λn bound state were performed in the data set of Pb–Pb collisions from 2010 ($13.8 \cdot 10^6$ minimum bias events) of ALICE. The H-dibaryon is a bound state of $uuddss$ ($\Lambda\Lambda$) and was first predicted by Jaffe in a bag model calculation [14]. Recent lattice QCD calculations [15,16] also suggest a bound state, with binding energies in the range 13–50 MeV. A chiral extrapolation of these lattice calculations to a physical pion mass resulted in an H-dibaryon unbound by either 13 ± 14 MeV [17] or close to the Ξp threshold [18]. The possible existence of a weakly bound H-dibaryon has been investigated via the decay channel $\mathrm{H} \to \Lambda + \mathrm{p} + \pi$. In the measured invariant mass distribution no signal is observed and an upper limit of $dN/dy \leq 2 \cdot 10^{-4}$ (99% CL) is obtained for a 1 MeV bound H-dibaryon. Also in the invariant mass distribution of deuterons and pions from displaced vertices, where a possible Λn bound state is expected to be visible, no signal can be seen. This yields in an upper limit of $dN/dy \leq 1.5 \cdot 10^{-3}$ (99% CL). The obtained upper limits are at least a factor 10 below different model predictions, see Fig. 4(b). More details on the searches of the two bound states (including the invariant mass distributions) can be found in [9].

5. Summary and conclusion

Production yields of light nuclei and their spectra have been measured in p–Pb (deuterons) and Pb–Pb (deuterons and ^{3}He) collisions. In addition, the loosely bound hypertriton has been observed and the production yield (divided by the B.R.) has been determined in Pb–Pb collisions. Two exotica, the weakly decaying bound states Λn and the H-dibaryon, are not observed in invariant mass analyses in Pb–Pb collisions and upper limits are given.

The production spectra of light nuclei can be understood based on the coalescence approach and also the increase of the deuteron-to-proton ratio with the charged particle multiplicity in

Fig. 2 is consistent with this picture. On the other hand the absolute production yields ($\mathrm{d}N/\mathrm{d}y$) of light nuclei and the hypertriton in Pb–Pb collisions are in good agreement with thermal model calculations, as shown in [12]. A thermal fit with or without including the measured nuclei and hypertriton yields leads to a temperature of 156 MeV in both cases. Thermal model predictions for the two weakly decaying bound states using this temperature of 156 MeV are a factor ten above the obtained upper limits for these states. Therefore the existence of the Λn bound state and H-dibaryon appears doubtful.

The presented measurements give a basis for the upcoming runs 2 and 3 where a high statistics sample will provide a better precision of the presented topics and open the field for searches for other forms of hyper-matter candidates [19].

References

[1] K. Aamodt, et al., J. Instrum. 3 (2008) S08002.
[2] A. Andronic, et al., Phys. Lett. B 697 (2011) 203.
[3] J. Cleymans, et al., Phys. Rev. C 84 (2011) 054916.
[4] J. Alme, et al., Nucl. Instrum. Methods A 622 (2010) 316.
[5] H. Bethe, Ann. Phys. 397 (1930) 325.
[6] A. Toia, for the ALICE Collaboration, Nucl. Phys. A 931 (2014) 315–319, these proceedings.
[7] B. Dönigus, J. Phys. Conf. Ser. 509 (2014) 012109.
[8] R. Scheibl, U. Heinz, Phys. Rev. C 59 (1999) 1585.
[9] B. Dönigus, Nucl. Phys. A 904–905 (0) (2013) 547c.
[10] B.I. Abelev, et al., Science 328 (2010) 58.
[11] J. Stachel, et al., J. Phys. Conf. Ser. 509 (2014) 012019.
[12] M. Floris, Nucl. Phys. A 931 (2014) 103–112, these proceedings.
[13] J.-F. Grosse-Oetringhaus, for the ALICE Collaboration, Nucl. Phys. A 931 (2014) 22–31, these proceedings.
[14] R.L. Jaffe, Phys. Rev. Lett. 38 (1977) 195.
[15] T. Inoue, et al., Phys. Rev. Lett. 106 (2011) 162002.
[16] S.R. Beane, et al., Phys. Rev. Lett. 106 (2011) 162001.
[17] P. Shanahan, et al., Phys. Rev. Lett. 107 (2011) 092004.
[18] J. Haidenbauer, U.-G. Meißner, Phys. Lett. B 706 (2011) 100.
[19] B. Abelev, et al., J. Phys. G, Nucl. Part. Phys. 41 (2014) 087001.